



LAWRENCE
LIVERMORE
NATIONAL
LABORATORY

Direct observation of electromagnetic Weibel filamentation in counter-streaming plasma flows

C. M. Huntington, F. Fiuza, J. S. Ross, A. Zylstra, R. P. Drake, G. Fiksel, D. H. Froula, G. Gregori, C. C. Kuranz, M. C. Levy, C. Li, J. Meinecke, T. Morita, R. Petrasso, C. Plechaty, B. A. Remington, D. D. Ryutov, Y. Sakawa, A. Spitkovsky, H. Takabe, H. S. Park

October 10, 2013

Nature Physics

Disclaimer

This document was prepared as an account of work sponsored by an agency of the United States government. Neither the United States government nor Lawrence Livermore National Security, LLC, nor any of their employees makes any warranty, expressed or implied, or assumes any legal liability or responsibility for the accuracy, completeness, or usefulness of any information, apparatus, product, or process disclosed, or represents that its use would not infringe privately owned rights. Reference herein to any specific commercial product, process, or service by trade name, trademark, manufacturer, or otherwise does not necessarily constitute or imply its endorsement, recommendation, or favoring by the United States government or Lawrence Livermore National Security, LLC. The views and opinions of authors expressed herein do not necessarily state or reflect those of the United States government or Lawrence Livermore National Security, LLC, and shall not be used for advertising or product endorsement purposes.

Direct observation of electromagnetic Weibel filamentation in counter-streaming plasma flows

C.M. Huntington¹, F. Fiuza¹, J. S. Ross¹, A. Zylstra², R. P. Drake³, G. Fiksel⁴, D. H. Froula⁴, G. Gregori⁵, C.C. Kuranz³, M. C. Levy¹, C. Li², J. Meinecke⁵, T. Morita⁶, R. Petrasso², C. Plechaty¹, B. A. Remington¹, D. D. Ryutov¹, Y. Sakawa⁶, A. Spitkovsky⁷, H. Takabe², H.-S. Park¹

¹*LLNL*

²*MIT*

³*Michigan*

⁴*LLE*

⁵*Oxford*

⁶*Osaka*

⁷*Princeton*

As the plasma ejecta from supernovae or other energetic astrophysical events streams through the interstellar media, it is shaped by instabilities that generate electric and magnetic fields. Specifically, counter-streaming plasmas are susceptible to the Weibel filamentation instability [1], which serves to generate electromagnetic fields on a range of scales [2]. The formation of current filaments coupled to transverse magnetic fields have been theorized to be responsible for the observed gamma-ray burst light curve [3], strong particle acceleration [4], and for providing seed fields for larger-scale cosmological magnetic structures [5]. While the presence of these instability-generated fields has been inferred from astrophysical observa-

tion and predicted in simulation, observation in experiments is challenging. Here we show, using charged particle (proton) probing, direct observation of filamentation-mediated magnetic fields in counter-streaming plasmas, fully consistent with 3-dimensional particle-in-cell (3D PIC) simulations and instability growth theory. The proton diagnostic also confirms the presence of self-organized magnetic field structures on large scales, consistent with previous observations [6]. Our results indicate that these features are produced by the $\nabla n \times \nabla T$ or Biermann battery effects in the initial plasma flows, and arise in PIC simulations through the incorporation of these fields at inception of the flows. The demonstration of Weibel-generated magnetic fields in counter-streaming plasmas is of fundamental importance to a wide range of astrophysical systems. Additionally, this demonstration of Weibel filamentation may serve as a platform for the investigation of a range of related phenomena, including jitter radiation [3] and large-scale magnetic field generation.

Our experiments were performed at the Omega Laser Facility [7], where two polyethylene (CH_2) plastic foils were laser-irradiated to generate high-velocity plasma flows (Fig. 1). The foils were oriented opposite each other and irradiated simultaneously, such that the expanding plasma flows interacted near the midplane between the foils. The plasma conditions in this experiment have been previously characterized under identical conditions with Thomson scattering [8]. When only a single foil was used, the plasma flow velocity was measured to exceed 1000 km/s, with an electron density of $5 \times 10^{18} \text{ cm}^{-3}$ and an electron and ion temperature less than 200 eV. When two opposing foils are used, as in the present work, the plasma density in the counter-propagating flows increased by the anticipated factor of 2, while the electron and ion temperatures increased

significantly due to a combination of collisional electron heating and ion two-stream instabilities [9].

It has long been known that instabilities in plasmas can generate magnetic fields even in the absence of seed fields. In seminal work, E. S. Weibel considered electromagnetic instability driven by the electron anisotropy at the background of resting ions [1]. The instability has a characteristic pattern, with numerous current filaments stretched along one of the axes of symmetry of the electron distribution function. Since this pioneering work, numerous analyses have discovered that such filamentation instabilities can be driven by a variety of sources of “free energy” in both non-relativistic and relativistic systems. In particular, ion instabilities in counter-streaming plasma flows have been conjectured to mediate the formation of collisionless shocks in non-magnetized plasmas [2, 3, 10, 11, 12], and to generate the electromagnetic turbulence necessary for cosmic ray acceleration in shocks [13]. This instability may also be responsible for the seed magnetic fields that are further amplified by astrophysical magnetic dynamo [4, 14]. The importance of Weibel and related filamentation instabilities in the dynamics of astrophysical systems makes laboratory experiments that can access the collisionless plasma regime particularly compelling.

In this experiment, the presence of magnetic fields are measured using proton probing. In the data shown here, protons were created by compressing a glass capsule filled with a 2:1 mixture of deuterium (D) and ³helium (³He) at a total pressure of 18 atm. At peak compression (10^{23} cm^{-3}), protons are produced quasi-isotropically at 14.7 MeV through fusion of D and ³He. The details of proton imaging have been treated at length [15] and proton probing has been used in numerous

high-energy-density experiments on OMEGA and elsewhere to image electric and magnetic field structures [16, 17, 18, 19, 20, 21]. The proton detector is positioned on the midplane of the CH₂ target foils such that the protons traverse the central interaction region, as shown in Fig. 1.

There are several striking features in the proton data, shown in Fig. 2 a). First, oriented along the flow direction is a pattern of filamentary structures, consistent with Weibel filamentation between the counter-propagating flows. These filaments span $\sim 700 \mu\text{m}$ above and below the midplane (0 on the y-axis of the image) and extend relatively uniformly over the horizontal field of view of the image. In addition to the filaments, two horizontal magnetic “plates” are seen above and below the midplane, producing bars of increased proton fluence approximately $400 \mu\text{m}$ apart. These large-scale magnetic features have been observed in previous experiments with similar geometries [6, 22], and are interpreted here as the result of the initial Biermann battery B-fields in the system. These fields are created at the target surface during the laser ablation [23] and are frozen in the flow, following the effective electron trajectory [24]. In the central region, the longitudinal electron velocity from the two flows is cancelled and the B-fields cannot readily cross the midplane, being mainly advected transversely and causing the formation of two magnetic plates [24].

In order to better understand both the Weibel- and Biermann battery-generated magnetic fields in the experimental system, we have conducted detailed 3D PIC simulations with the code OSIRIS [25] to model the counter-streaming plasma flows and the generation of EM fields from first principles. The flows are initialized with the properties measured experimentally in the mid-

plane region, namely each flow has $n_e = 5 \times 10^{18} \text{ cm}^{-3}$, $v_e = v_i = 1000 \text{ km/s}$, and $T_e = T_i = 100 \text{ eV}$. Figures 3a and 3b show the B-field structure $\sim 2 \text{ ns}$ after the flows begin interacting, at approximately the time that the experimental data was collected. As the current filamentation instability grows, we observe clear filamentary structure in the midplane where plasma interpenetration occurs. The magnetic energy associated with the instability growth is driven by the ion flows and goes mainly into the transverse component of the field, as expected from the instability analysis. The amplitude of these B-fields grows exponentially during the linear phase, with a growth rate of $\sim 0.2 v/c \omega_{pi}^{-1}$ or $1/\Gamma = 0.5 \text{ ns}$, which is consistent with the linear theory of the instability (see Figure 3c and the caption discussion). The linear phase of the instability saturates after 1 - 1.5 ns of interaction (i.e. after ~ 2 -3 e-foldings). After 2 ns, the filaments are approximately $\sim 400 \mu\text{m}$ in diameter, which is consistent with experimental observations. In the subsequent nonlinear phase, the B-field amplitude continues to increase; the ratio of spatially-averaged magnetic energy to the kinetic energy of the flows reaches $> 1\%$ by the end of the interaction (Fig. 3c). Locally, the B-fields reach peak amplitudes of 0.32 MG, which corresponds to a magnetic energy density that is 5% of the kinetic energy density of the flows. These high values illustrate the power of this collisionless instability in converting kinetic energy into electromagnetic energy. The large-amplitude B-fields cause the deflection of the incoming flows and the randomization of their kinetic energy. At time scales longer than those addressed here, this can also lead to the formation of shock waves and to particle acceleration from these shocks [13, 26].

Simulations were also used to investigate the role of Biermann battery B-fields generated by the $\nabla n \times \nabla T$ term near the surface of the foils during the laser interaction. Using the plasma

described above, we have immersed the flows in large-scale B-fields with a peak amplitude of 50 kGauss [22, 27]. In keeping with the geometry of the gradients of n and T in the system, the fields are made to encircle the initial plasma flows. Because the electron density in the simulations does not diverge transversely at the midplane as in the experiment [24], the fields are initialized only in the leading edge of the flow, ensuring that the B-field in the interaction region does not grow unbounded. The addition of these fields leads to a long-range order in the system, and results in the the magnetic plates seen in the data (Fig. 2 a). The presence of this field does not affect considerably the formation of the ion Weibel instability, as the ions remain unmagnetized. This is supported by simulations where the initial B-fields associated with the Biermann battery are not included, in which case the structure and evolution of the Weibel-generated field is essentially the same (see Figure 3c).

To more readily compare the PIC results with the experiments, we have produced synthetic proton radiographs from the B-field structure in the simulations. As in the experiment, a source of 14.7 MeV protons is generated with a phase-space distribution corresponding to an isotropic point source located 1 cm away from the beginning of the simulation box. The protons probe the self-consistent field structure, and then are ballistically propagated to a 13 cm \times 13 cm detector plane 30 cm from the source (identical geometry as the OMEGA experiments). The simulated proton radiography is shown in Figure 2b), and is in good agreement with the experimental data. To verify the mechanisms for the plate and filament features in the image, the field strength was selectively varied in the simulation. This confirmed that the observed filamentary structure in the central region of the image is associated with the Weibel B-fields, whereas the two vertical plates

are associated with the Biermann battery fields.

To assess the susceptibility of the plasma in our experiment to Weibel growth, we have performed a linear stability analysis based on the collisionless Vlasov equation. Using the same techniques as in the earlier studies [28, 29], we arrived at the dispersion relation properly accounting for the chemical composition of the flow. Such a description is necessary for multi-species plasmas (the present system consists of carbon and hydrogen), and represents a new aspect to the dispersion relation calculation. Additional details are included in Supplemental Information; the results are presented in Fig. 3d). The linear growth-rate for the temperature of ~ 1 keV is sufficient for the mode to grow to a well-developed state during the first 1-2 ns of interaction between the plasma flows, as seen in both experiment and simulation.

Using proton radiography to probe the system, it is clear that self-generated magnetic fields from a multitude of sources, including Weibel instability and Biermann battery effects, shape the evolution of the plasma in these experiments. The ability of 3D simulations to model the instability growth, paired with the generation of synthetic proton images via self-consistent projection of charged particles through the PIC fields, allows for a powerful, direct comparison to data. The importance of magnetic fields over range of spatial scales in numerous astrophysical systems make these experiments an exciting test bed the study of self-generated magnetic fields in plasmas.

Acknowledgements We thank the staff of the OMEGA laser facility for their experimental support. This work was performed under the auspices of the US Department of Energy by the Lawrence Livermore National Laboratory, under Contract No. DE-AC52-07NA27344. Further support was provided by

LLNL LDRD grant No. 11-ERD-054 and the International Collaboration for High Energy Density Science (ICHEDS), supported by the Core-to-Core Program of the Japan Society for the Promotion of Science. The research leading to these results received funding from the European Research Council under the European Communitys Seventh Framework Programme (FP7/2007-2013), ERC grant agreement numbers 256973 and 247039.

Competing Interests The authors declare that they have no competing financial interests.

Correspondence Correspondence and requests for materials should be addressed to C. M. Huntington. (email: huntington4@llnl.gov).

1. Erich S. Weibel. Spontaneously growing transverse waves in a plasma due to an anisotropic velocity distribution. *Phys. Rev. Lett.*, 2:83–84, Feb 1959.
2. Y. Kazimura, J. I. Sakai, T. Neubert, and S. V. Bulanov. Generation of a small-scale quasi-static magnetic field and fast particles during the collision of electron-positron plasma clouds. *The Astrophysical Journal Letters*, 498(2):L183, 1998.
3. M. V. Medvedev, D. Lazzati, B. C. Morsony, and J. C. Workman. Jitter radiation as a possible mechanism for gamma-ray burst afterglows: spectra and light curves. *Astrophys J.*, 666, 2007. JILA Pub. 8044.
4. K.-I. Nishikawa, J. Niemiec, P. E. Hardee, M. Medvedev, H. Sol, Y. Mizuno, B. Zhang, M. Pohl, M. Oka, and D. H. Hartmann. Weibel instability and associated strong fields in a

- fully three-dimensional simulation of a relativistic shock. *The Astrophysical Journal Letters*, 698(1):L10, 2009.
5. Reinhard Schlickeiser. On the origin of cosmological magnetic fields by plasma instabilities. *Plasma Physics and Controlled Fusion*, 47(5A):A205, 2005.
 6. N. L. Kugland, D. D. Ryutov, P-Y. Chang, R. P. Drake, G. Fiksel, D. H. Froula, S. H. Glenzer, G. Gregori, M. Grosskopf, M. Koenig, Y. Kuramitsu, C. Kuranz, M. C. Levy, E. Liang, J. Meinecke, F. Miniati, T. Morita, A. Pelka, C. Plechaty, R. Presura, A. Ravasio, B. A. Remington, B. Reville, J. S. Ross, Y. Sakawa, A. Spitkovsky, H. Takabe, and H-S. Park. Self-organized electromagnetic field structures in laser-produced counter-streaming plasmas. *Nature Physics*, 8(11):809–812, 2012.
 7. T. R. Boehly, R. S. Craxton, T. H. Hinterman, J. H. Kelly, T. J. Kessler, S. A. Kumpan, S. A. Letzring, R. L. McCrory, S. F. B. Morse, W. Seka, S. Skupsky, J. M. Soures, and C. P. Verdon. The upgrade to the omega laser system. volume 66, pages 508–510. AIP, 1995.
 8. J. S. Ross, S. H. Glenzer, P. Amendt, R. Berger, L. Divol, N. L. Kugland, O. L. Landen, C. Plechaty, B. Remington, D. Ryutov, W. Rozmus, D. H. Froula, G. Fiksel, C. Sorce, Y. Kuramitsu, T. Morita, Y. Sakawa, H. Takabe, R. P. Drake, M. Grosskopf, C. Kuranz, G. Gregori, J. Meinecke, C. D. Murphy, M. Koenig, A. Pelka, A. Ravasio, T. Vinci, E. Liang, R. Presura, A. Spitkovsky, F. Miniati, and H.-S. Park. Characterizing counter-streaming interpenetrating plasmas relevant to astrophysical collisionless shocks. *Physics of Plasmas*, 19(5):056501, 2012.

9. J. S. Ross, H.-S. Park, R. Berger, L. Divol, N. L. Kugland, W. Rozmus, D. Ryutov, and S. H. Glenzer. Collisionless coupling of ion and electron temperatures in counterstreaming plasma flows. *Phys. Rev. Lett.*, 110:145005, Apr 2013.
10. S S Moiseev and R Z Sagdeev. Collisionless shock waves in a plasma in a weak magnetic field. *Journal of Nuclear Energy. Part C, Plasma Physics, Accelerators, Thermonuclear Research*, 5(1):43, 1963.
11. Mikhail V. Medvedev and Abraham Loeb. Generation of magnetic fields in the relativistic shock of gamma-ray burst sources. *The Astrophysical Journal*, 526(2):697, 1999.
12. A. Gruzinov and E. Waxman. Gamma-ray burst afterglow: Polarization and analytic light curves. *Astrophys. J.*, 511:852–861, Feb 1999.
13. Anatoly Spitkovsky. Particle acceleration in relativistic collisionless shocks: Fermi process at last? *The Astrophysical Journal Letters*, 682(1):L5, 2008.
14. Russell M. Kulsrud, Renyue Cen, Jeremiah P. Ostriker, and Dongsu Ryu. The protogalactic origin for cosmic magnetic fields. *The Astrophysical Journal*, 480(2):481, 1997.
15. N. L. Kugland, D. D. Ryutov, C. Plechaty, J. S. Ross, and H.-S. Park. Invited article: Relation between electric and magnetic field structures and their proton-beam images. *Review of Scientific Instruments*, 83(10):101301, 2012.
16. C K Li, F H Séguin, J A Frenje, M Rosenberg, A B Zylstra, R D Petrasso, P A Amendt, J A Koch, O L Landen, H S Park, H F Robey, R P J Town, A Casner, F Philippe, R Betti, J P

- Knauer, D D Meyerhofer, C A Back, J D Kilkenny, and A Nikroo. Diagnosing indirect-drive inertial-confinement-fusion implosions with charged particles. *Plasma Physics and Controlled Fusion*, 52(12):124027, 2010.
17. C. K. Li, D. G. Hicks, F. H. Séguin, J. A. Frenje, R. D. Petrasso, J. M. Soures, P. B. Radha, V. Yu. Glebov, C. Stoeckl, D. R. Harding, J. P. Knauer, R. Kremens, F. J. Marshall, D. D. Meyerhofer, S. Skupsky, S. Roberts, C. Sorce, T. C. Sangster, T. W. Phillips, M. D. Cable, and R. J. Leeper. D ³He proton spectra for diagnosing shell rho r and fuel t[sub i] of imploded capsules at omega. *Physics of Plasmas*, 7(6):2578–2584, 2000.
 18. A. J. Mackinnon, P. K. Patel, R. P. Town, M. J. Edwards, T. Phillips, S. C. Lerner, D. W. Price, D. Hicks, M. H. Key, S. Hatchett, S. C. Wilks, M. Borghesi, L. Romagnani, S. Kar, T. Toncian, G. Pretzler, O. Willi, M. Koenig, E. Martinolli, S. Lepape, A. Benuzzi-Mounaix, P. Audebert, J. C. Gauthier, J. King, R. Snavely, R. R. Freeman, and T. Boehlly. Proton radiography as an electromagnetic field and density perturbation diagnostic (invited). *Review of Scientific Instruments*, 75(10):3531–3536, 2004.
 19. J. R. Rygg, F. H. Séguin, C. K. Li, J. A. Frenje, M. J.-E. Manuel, R. D. Petrasso, R. Betti, J. A. Delettrez, O. V. Gotchev, J. P. Knauer, D. D. Meyerhofer, F. J. Marshall, C. Stoeckl, and W. Theobald. Proton radiography of inertial fusion implosions. *Science*, 319(5867):1223–1225, 2008.
 20. L. Willingale, P. M. Nilson, M. C. Kaluza, A. E. Dangor, R. G. Evans, P. Fernandes, M. G. Haines, C. Kamperidis, R. J. Kingham, C. P. Ridgers, M. Sherlock, A. G. R. Thomas, M. S.

- Wei, Z. Najmudin, K. Krushelnick, S. Bandyopadhyay, M. Notley, S. Minardi, M. Tatarakis, and W. Rozmus. Proton deflectometry of a magnetic reconnection geometry. *Physics of Plasmas*, 17(4):043104, 2010.
21. A. B. Zylstra, C. K. Li, H. G. Rinderknecht, F. H. Séguin, R. D. Petrasso, C. Stoeckl, D. D. Meyerhofer, P. Nilson, T. C. Sangster, S. Le Pape, A. Mackinnon, and P. Patel. Using high-intensity laser-generated energetic protons to radiograph directly driven implosions. *Review of Scientific Instruments*, 83(1):013511, 2012.
22. N. L. Kugland, J. S. Ross, P.-Y. Chang, R. P. Drake, G. Fiksel, D. H. Froula, S. H. Glenzer, G. Gregori, M. Grosskopf, C. Huntington, M. Koenig, Y. Kuramitsu, C. Kuranz, M. C. Levy, E. Liang, D. Martinez, J. Meinecke, F. Miniati, T. Morita, A. Pelka, C. Plechaty, R. Presura, A. Ravasio, B. A. Remington, B. Reville, D. D. Ryutov, Y. Sakawa, A. Spitkovsky, H. Takebe, and H.-S. Park. Visualizing electromagnetic fields in laser-produced counter-streaming plasma experiments for collisionless shock laboratory astrophysics. *Physics of Plasmas*, 20(5):056313, 2013.
23. J. A. Stamper, E. A. McLean, and B. H. Ripin. Studies of spontaneous magnetic fields in laser-produced plasmas by faraday rotation. *Phys. Rev. Lett.*, 40:1177–1181, May 1978.
24. D. D. Ryutov, N. L. Kugland, M. C. Levy, C. Plechaty, J. S. Ross, and H. S. Park. Magnetic field advection in two interpenetrating plasma streams. *Physics of Plasmas*, 20(3):032703, 2013.
25. R. Fonseca, L. Silva, F. Tsung, V. Decyk, W. Lu, C. Ren, W. Mori, S. Deng, S. Lee, T. Kat-

- souleas, and J. Adam. Osiris: A three-dimensional, fully relativistic particle in cell code for modeling plasma based accelerators. In Peter Sloot, Alfons Hoekstra, C. Tan, and Jack Dongarra, editors, *Computational Science, ICCS 2002*, volume 2331 of *Lecture Notes in Computer Science*, pages 342–351. Springer Berlin / Heidelberg, 2002.
26. S. F. Martins, R. A. Fonseca, L. O. Silva, and W. B. Mori. Ion dynamics and acceleration in relativistic shocks. *The Astrophysical Journal Letters*, 695(2):L189, 2009.
27. M. G. Haines. Magnetic-field generation in laser fusion and hot-electron transport. *Canadian Journal of Physics*, 64(8):912–919, 1986.
28. Ronald C. Davidson, David A. Hammer, Irving Haber, and Carl E. Wagner. Nonlinear development of electromagnetic instabilities in anisotropic plasmas. *Physics of Fluids*, 15(2):317–333, 1972.
29. R. L. Berger, J. R. Albritton, C. J. Randall, E. A. Williams, W. L. Kruer, A. B. Langdon, and C. J. Hanna. Stopping and thermalization of interpenetrating plasma streams. *Physics of Fluids B: Plasma Physics*, 3(1):3–12, 1991.

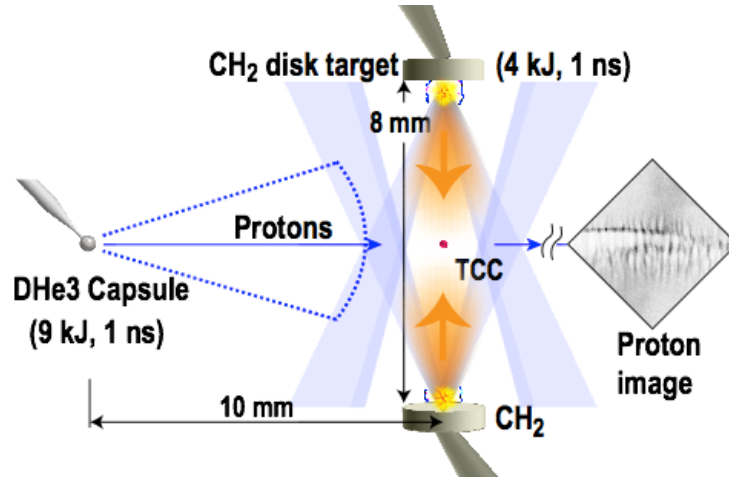


Figure 1: Experimental configuration of opposing flow measurements on OMEGA. In this geometry, a pair of polyethylene (CH_2) plastic foils of diameter 2 mm and thickness $500 \mu\text{m}$ were separated by 8 mm along a common vector. Each was irradiated with 8 overlapped laser beams delivering ≈ 4 kJ of 351 nm laser energy in a 1 ns square pulse. Phase plates were used to produce super-gaussian laser spots with focal spot diameters of $250 \mu\text{m}$ on the target surface. In the midplane between the plastic disks, a capsule filled with a mix of deuterium and ^3He gases was irradiated by 18 beams (≈ 9 kJ total laser energy), compressing it and producing an isotropic burst of 14.7 MeV of protons upon stagnation. The capsule was located 1 cm from the center point between the foils, and the protons were recorded after transiting the plasma interaction region using a CR39 detector located 30 cm from the proton source.

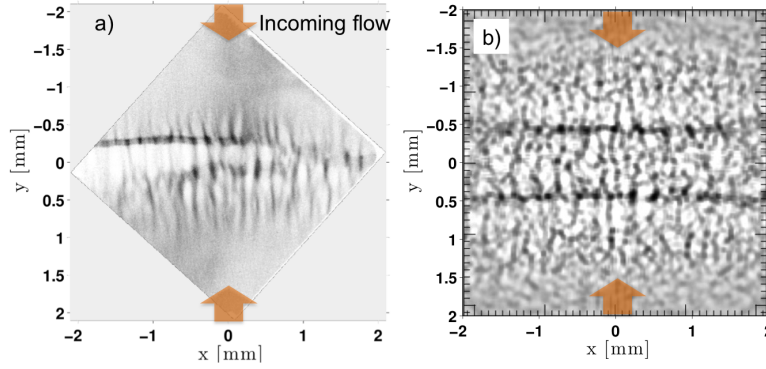


Figure 2: Experimental data (a) and synthetic proton radiography from post-processed PIC simulations (b). In both cases the plasma flows enter the frame from the top and bottom. Extended, coherent magnetic “plates” are formed above and below the midplane as a result of the large-scale Biermann battery fields generated in the laser ablation process. Superposed are the protons deflected from Weibel filaments, which appear at the image with a spatial period of $\sim 250 \mu\text{m}$ in both the data and simulation. Notably, the spacing of filaments in the plasma is larger than this measured spacing in the radiograph, as a result of multiple deflections that the protons experience as they traverse the 3D “forest” of filaments. This result is discussed further in the Supplemental information section.

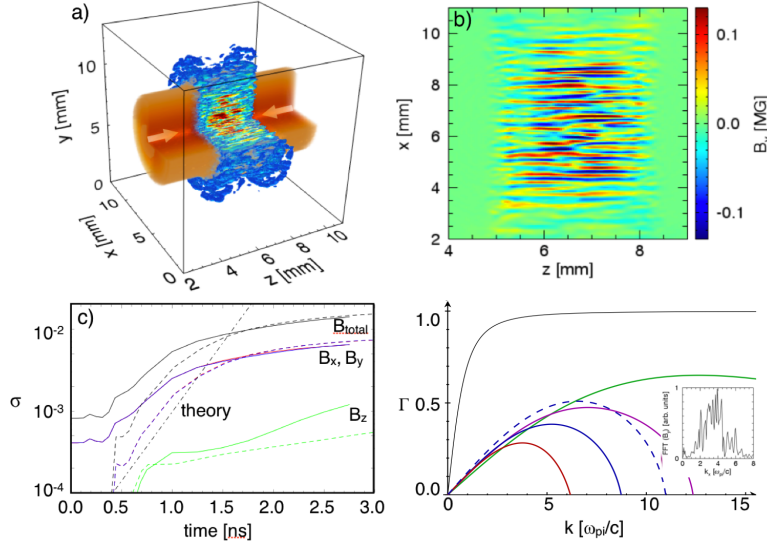


Figure 3: a) 3D OSIRIS simulation of the system after 2 ns of interaction between the counter-streaming plasma flows. Magnetic fields are shown in the blue/red color scale, with electron density in orange. b) Magnetic field slice along the y-axis midplane, illustrating the presence of strong filaments associated with the Weibel instability. c) Plasma magnetization σ as a function of time. The case of zero initial B-field is shown in solid lines, whereas the case of initial Biermann battery field is represented by the dashed lines. The (green, blue, red) lines show the (x,y,z) components of the B-field and the total B-field is shown in black. The dot-dashed line show the theoretical growth rate of the ion Weibel instability. d) The linear Weibel growth rate Γ [$\omega_{pi}v/c$] vs the wave number k [ω_{pi}/c]. The velocity of each stream is 10^8 cm/s (the directed energy of the carbon ions is then ≈ 60 keV). The green, blue and red curves correspond to CH_2 flows at electron and ion temperatures of 0.1 keV (green), 0.5 keV (magenta), 1 keV (blue) and 2 keV (red). The maximum growth rate for the electron density of 10^{19} cm^{-3} in the CH_2 plasma is 0.5×10^{10} s^{-1} for blue curve. The dashed blue curve is for pure carbon at $T_e = T_i = 1$ keV. The difference between the solid and dashed blue curves is a manifestation of stabilization by the light ions. The black curve is a reference growth rate $\Gamma = k v \omega_{pi} / \sqrt{k^2 c^2 + \omega_{pi}^2}$. Finally, the inset plot shows mode distribution of the magnetic field in k -space from simulation after 2ns of interaction, showing a range of unstable k consistent with the theoretical analysis.